

**Te-RICH CANFIELDITE,  $\text{Ag}_8\text{Sn}(\text{S},\text{Te})_6$ , FROM THE LENGENBACH QUARRY,  
BINNTAL, CANTON VALAIS, SWITZERLAND: OCCURRENCE,  
DESCRIPTION AND CRYSTAL STRUCTURE**

LUCA BINDI §

*Museo di Storia Naturale, Sezione Mineralogia e Litologia, Università degli Studi di Firenze,  
Via G. La Pira 4, I-50121 Firenze, Italy, and CNR – Istituto di Geoscienze e Georisorse, Sezione di Firenze,  
Via G. La Pira 4, I-50121 Firenze, Italy*

FABRIZIO NESTOLA

*Dipartimento di Geoscienze, Università degli Studi di Padova, Via Gradenigo 6, I-35131 Padova, Italy*

ALESSANDRO GUASTONI

*Museo di Mineralogia, Università degli Studi di Padova, Palazzo Cavalli, Via Matteotti 30, I-35121, Padova, Italy*

FEDERICO ZORZI

*Dipartimento di Geoscienze, Università degli Studi di Padova, Via Gradenigo 6, I-35131 Padova, Italy*

LUCA PERUZZO

*CNR – Istituto di Geoscienze e Georisorse, Sezione di Padova, Via Gradenigo 6, I-35131 Padova, Italy*

THOMAS RABER

*Edith-Stein-Str. 9, D-79110 Freiburg, Germany*

ABSTRACT

In order to evaluate the effects of Te-for-S substitution in the minerals of the argyrodite group, the crystal structure and chemical composition of a crystal of Te-rich canfieldite from the Lengenbach quarry, Binntal, Switzerland, was investigated. The unit-cell parameters are  $a$  11.0003(6) Å and  $V$  1331.1(1) Å<sup>3</sup>. The structure was solved and refined in the space group  $F\bar{4}3m$  to  $R_1 = 0.0308$  for 194 independent reflections and 21 parameters. Quantitative analysis led to the chemical formula  $\text{Ag}_{8.05}(\text{Sn}_{1.03}\text{Ge}_{0.01})_{\Sigma 1.04}(\text{S}_{3.95}\text{Te}_{1.95}\text{Se}_{0.01})_{\Sigma 5.91}$ , ideally  $\text{Ag}_8\text{Sn}(\text{S},\text{Te})_6$ . The crystal structure of Te-rich canfieldite was found to be topologically identical to that of putzite,  $(\text{Cu}_{4.7}\text{Ag}_{3.3})\text{GeS}_6$ . Neglecting the short Ag-Ag contacts (due to disorder), the two Ag atoms in the structure can be considered as three-fold (Ag1) and four-fold (Ag2) coordinated. Tin adopts a regular tetrahedral coordination. The refinement of the site-occupancy factor indicates Te to be disordered over the three anion positions (*i.e.*, X1, X2, and X3), with a preference for the X1 site.

*Keywords:* canfieldite; argyrodite; putzite; tellurium; crystal structure; chemical composition, Lengenbach, Switzerland.

INTRODUCTION

The minerals of the argyrodite group consist primarily of three members: argyrodite ( $\text{Ag}_8\text{GeS}_6$ ), canfieldite ( $\text{Ag}_8\text{SnS}_6$ ), and putzite  $[(\text{Cu}_{4.7}\text{Ag}_{3.3})\text{GeS}_6]$ .

Argyrodite and canfieldite have been found to contain appreciable amounts of Te replacing S. The existence of Te-bearing canfieldite has been reported from several localities: Revelstoke, Canada (Harris & Owens 1971), Belukhinskoye, Russia (Ontoyev *et al.* 1971), the

§ E-mail address: luca.bindi@unifi.it

Tsumo, Kuga, and Nakatatsu mines, Japan (Soeda *et al.* 1984, Kikuchi *et al.* 1980, Marioko 1981, respectively), Zlata Bana, Slovakia (Duda & Kristin 1978), and the Cirotan mine, Indonesia (Milési *et al.* 1994). Tellurium-bearing argyrodite has been recently described by Tămaş *et al.* (2006) from samples from silver-rich, gold-poor veins from the Roşia Montană ore deposit, South Apuseni Mountains, Romania. On the basis of chemical and powder X-ray data, Harris & Owens (1971) proposed that Te replaces S in the structure of canfieldite, yielding an ideal formula of  $\text{Ag}_8\text{Sn}(\text{S},\text{Te})_6$ .

According to Wang (1978), argyrodite and canfieldite are isostructural (space group  $Pna2_1$  or  $Pnam$ ) and a solid solution exists between these two minerals. However, only the crystal structure of argyrodite has been published (Eulenberger 1977), and no structural studies of natural canfieldite have been carried out to date. On the other hand, several structural studies of synthetic argyrodite-type compounds have been reported, mainly because such phases are of interest for their manifold structural and physical properties, for example, as electrolytes (*e.g.*, Evain *et al.* 1998, Gaudin *et al.* 2001, Rao & Adams 2011). These compounds undergo three phase transitions: the high-temperature phase crystallizes in the space group  $F43m$ ; the medium-temperature phase, usually refined using a non-harmonic technique (see Evain *et al.* 1998 for an explanation), has the space group  $P2_13$ ; and the low-temperature phase has apparent space-group  $F43m$ , but actually adopts an orthorhombic symmetry (space groups  $Pna2_1$ ,  $Pnam$  or  $Pmn2_1$ ).

The present study was undertaken in order to provide a crystal-chemical characterization of Te-rich canfieldite from the Lengenbach quarry and to clarify the structural role of tellurium in these minerals.

#### OCCURRENCE

The sample containing Te-rich canfieldite was collected by one of the authors (TR) at the Lengenbach quarry in 1993. Tellurium-rich canfieldite is hosted in a centimetric tennantite matrix (Fig. 1). It does not show obvious forms of twinning or any inclusions of, or intergrowths with, other minerals. The mineral assemblage also includes seligmannite, thalcosite, wurtzite, jordanite, and galena.

The Lengenbach Pb, Tl, Ag, As, Sb, Hg, and Ba mineralization, hosted in Triassic dolomitic marbles, is characterized by appreciable geochemical enrichments in Pb-Tl-As-S (Graeser 1965, Hofmann & Knull 1996). Over the nearly 200 years of quarrying activity at this locality, over 100 mineral specimens have been described, including 28 type-locality minerals (Graeser *et al.* 2008, Nestola *et al.* 2010). Note that neither geochemical nor mineralogical data have ever mentioned the presence of tellurium-bearing minerals at Lengenbach. Thus, Te-rich canfieldite, other than representing a new species to add to the list of minerals for this locality, also represents the first tellurium-bearing mineral described so far at the Lengenbach quarry.

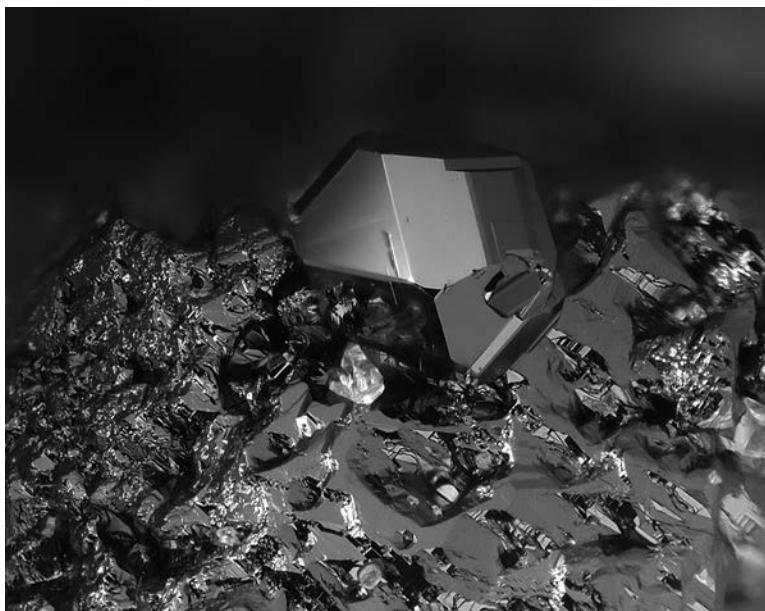


FIG. 1. Macroscopic image of Te-rich canfieldite. The image view is 0.8 mm.

## CHEMICAL COMPOSITION

A preliminary SEM study carried out with a CamScan MX2500 scanning electron microscope, equipped with a LaB<sub>6</sub> cathode, four quadrant solid-state BSE detector and a EDAX EDS system for microanalysis, did not indicate the presence of elements ( $Z > 9$ ) other than Ag, Sn, S, Te, and minor Cu, Ge, Zn, and Se. The analytical conditions were: accelerating voltage of 20 kV, filament emission of  $\sim 130 \mu\text{A}$  and working distance of 30 mm.

The chemical composition was then determined using wavelength-dispersive analysis (WDS) by means of a CAMECA-CAMEBAX electron microprobe. Concentrations of major and minor elements were determined with a fine-focus beam ( $\sim 1 \mu\text{m}$ ) at an accelerating voltage of 20 kV and a beam current of 20 nA, with 10 s counting times for peak and 5 s for total background. For the WDS analyses the following lines were used: AgK $\alpha$ , SnK $\alpha$ , SK $\alpha$ , TeK $\alpha$ , CuL $\alpha$ , GeL $\alpha$ , ZnL $\alpha$ , and SeL $\beta$ . X-ray counts were converted into elements wt.% using the PAP correction program (Pouchou & Pichoir 1985). The standards employed were native elements for Cu, Ag, Te, Se, Ge, sphalerite for S and Zn, and SnO<sub>2</sub> for Sn. The crystal fragment was found to be homogeneous within analytical error. The average chemical composition (11 analyses of different spots) and the ranges of wt.% of elements are reported in Table 1. On the basis of 15 atoms, the chemical formula can be written as Ag<sub>8.05</sub>(Sn<sub>1.03</sub>Ge<sub>0.01</sub>) $\Sigma$ 1.04(S<sub>3.95</sub>Te<sub>1.95</sub>Se<sub>0.01</sub>) $\Sigma$ 5.91 or, ideally, as Ag<sub>8</sub>Sn(S,Te)<sub>6</sub>.

## X-RAY CRYSTALLOGRAPHY

Three crystals of Te-rich canfieldite were selected from the rock sample and examined by means of a

TABLE 1. ELECTRON MICROPROBE DATA (MEANS AND RANGES IN WT. %) AND ATOMS PER FORMULA UNIT (ON THE BASIS OF 15 ATOMS) WITH THEIR STANDARD DEVIATIONS ( $\sigma$ ) FOR Te-RICH CANFIELDITE

	Mean	Ranges	Ratios	( $\sigma$ )
Ag	63.26	62.92 – 63.76	8.05	(0.16)
Cu	0.01	0.00 – 0.05	0.00	(0.00)
Sn	8.88	8.59 – 9.08	1.03	(0.03)
Ge	0.04	0.00 – 0.15	0.01	(0.01)
Zn	0.03	0.00 – 0.08	0.00	(0.00)
S	9.23	9.15 – 9.37	3.95	(0.09)
Se	0.05	0.02 – 0.09	0.01	(0.01)
Te	18.15	17.80 – 18.53	1.95	(0.05)
Total	99.65	99.05 – 100.32	15.00	

STOE-STADI IV CCD single-crystal diffractometer using graphite-monochromatized MoK $\alpha$  radiation. For all the crystals investigated, nearly identical cubic unit-cell values ( $a \sim 11.00 \text{ \AA}$ ) were found. Data collection was carried out using the crystal showing the best diffraction quality (see Table 2 for details). Intensity integration and standard Lorentz-polarization correction were performed with the CrysAlis (Oxford Diffraction) software package. The programs X-RED and X-SHAPE (STOE & CIE) were used for the absorption correction. The statistical tests on the distribution of  $|E|$  values ( $|E^2 - 1| = 0.653$ ), which did not indicate the presence of an inversion centre, together with the observed systematic absences and the good agreement of reflections in the Laue class  $m\bar{3}m$ , led to the choice of one of the following space groups:  $F432$ ,  $F\bar{4}3m$  or  $Fm\bar{3}m$ . Since one of the characteristic structural features

TABLE 2. CRYSTALLOGRAPHIC DATA AND REFINEMENT PARAMETERS FOR Te-RICH CANFIELDITE

Crystal data	
Ideal formula	Ag <sub>8</sub> Sn(S,Te) <sub>6</sub>
Crystal system	cubic
Space group	$F43m$ (#216)
Unit-cell parameter $a$ (Å)	11.0003(6)
Unit-cell volume (Å <sup>3</sup> )	1331.1(1)
Z	4
Crystal size (mm)	0.160×0.160×0.140
Data collection	
Diffractometer	STOE-STADI IV CCD
Temperature (K)	298(3)
Radiation, wavelength (Å)	MoK $\alpha$ , 0.71073
2 $\theta$ max for data collection (°)	55.54
Crystal-detector dist. (mm)	50
$h, k, l$ ranges	$\pm 14, \pm 14, \pm 14$
Axis, frames, width (°), time per frame (s)	$\omega$ - $\varphi$ , 1380, 1.00, 25
Total reflections collected	13824
Unique reflections ( $R_{int}$ )	194 (0.131)
Unique reflections $F > 4\sigma(F)$	191
Data completeness to $\theta_{max}$ (%)	99.2
Absorption correction method	X-RED and X-SHAPE
Structure refinement	
Refinement method	Full-matrix least-squares on $F^2$
Weighting scheme	$1/\sigma^2(F)$
Data/restraints/parameters	191/0/21
Extinct. coefficient	0.0002(1)
$R_1$ [ $F > 4\sigma(F)$ ], $wR_2$ [ $F > 4\sigma(F)$ ]	0.0308, 0.0565
$R_1$ all, $wR_2$ all	0.0308, 0.0565
Goodness-of-fit on $F^2$	1.660
Largest diff. peak and hole ( $e^-/\text{\AA}^3$ )	1.39, -2.00
$R_w = (n/n-1)^{1/2} [F_o^2 - F_c^2(\text{mean})^2] \sum F_o^2$ $R_1 = \sum   F_o  -  D_c   / \sum  F_o $ $wR_2 = \left[ \sum [w(F_o^2 - F_c^2)^2] / \sum [w(F_o^2)^2] \right]^{1/2}$ $GoodF = \left[ \sum [w(F_o^2 - F_c^2)^2] / (n - \rho) \right]^{1/2}$ where $n$ = no. of reflections, $\rho$ = no. of refined	

of argyrodite-group compounds is the occurrence of so-called supertetrahedra (see Paar *et al.* 2004 and references therein), which (in cubic symmetry) can only realized by a  $\bar{4}$  operation, other space groups (without  $\bar{4}$ ), permissible on the basis of systematic absences, could be rejected. Thus, the crystal structure was solved in the  $F\bar{4}3m$  space group. The positions of most of the atoms (all the metals and one anion) were determined from the three-dimensional Patterson synthesis (Sheldrick 2008). A least-squares refinement using these heavy-atom positions and isotropic temperature factors yielded an  $R_1$  factor of 0.0912. Three-dimensional difference Fourier synthesis yielded the positions of the remaining anions. The full-matrix least-squares program SHELXL-97 (Sheldrick 2008) was used for the refinement of the structure. The introduction of anisotropic-temperature factors for all the atoms led to  $R_1 = 0.0696$ . The site occupancies of all the positions was allowed to vary using different couples of neutral Sn, Ag, S, and Te scattering curves (Ibers & Hamilton 1974). Given the disorder observed in the structure, the Ag1 and Ag2 positions [separation 1.113(1) Å] were found to be partially occupied, but an equation was added on the global Ag occupancy to fulfil the overall charge-balance (*i.e.*, Ag = 8.00 a.p.f.u. for Z = 4). The final results are given in Table 3. At the final stage, with anisotropic atomic displacement parameters for all atoms and no constraints, the residual value settled at  $R_1 = 0.0308$  for 191 observed reflections [ $F_o > 4\Sigma(F_o)$ ] and 21 refined parameters and at  $R_1 = 0.0308$  for all 194 independent reflections. Inspection of the difference-Fourier map

revealed that maximum positive and negative peaks were 1.39 and 2.00  $e/\text{Å}^3$ , respectively. Fractional atom coordinates and anisotropic-displacement parameters are shown in Table 3. Bond distances are reported in Table 4. The calculated X-ray powder pattern is given in Table 5. A list of the observed and calculated structure factors is available from the Depository of Unpublished Data, MAC website [document Te-Rich Canfieldite CM50\_111].

#### DESCRIPTION OF THE STRUCTURE

The crystal structure of Te-rich canfieldite (Fig. 2) is topologically identical to that of putzite (Paar *et al.* 2004) and the synthetic  $\text{Cu}_8\text{GeS}_6$  cubic compound (Ishii *et al.* 1999). From a topological point of view, it can be seen as based on regular polyhedra such as  $\text{Sn}(X)_4$ ,  $(X)\text{Ag}_6$ ,  $(X)\text{Ag}_{12}$ , and  $(X)\text{Ag}_{12}$ , where  $X = (\text{S}, \text{Te})$ . Alternatively, neglecting the short Ag-Ag contacts (due to disorder), the Ag1 atom may be considered as three-fold coordinated (Fig. 3) with a mean Ag-X distance of 2.53 Å, in good agreement with (1) the Ag-S distance found for the Ag(1) position in the crystal structure of stephanite,  $\text{Ag}_5[\text{S}(\text{SbS}_3)]$  (2.54 Å; Ribár & Nowacki 1970); (2) the mean distance found for the Ag position in the crystal structure of pyrargyrite,  $\text{Ag}_3[\text{SbS}_3]$  (2.57 Å; Engel & Nowacki 1966), and (3) the mean distances found for the silver atoms in a close to triangular coordination in the pearceite-polybasite group of minerals (range: 2.59-2.60 Å; Bindi *et al.* 2006, 2007, Evain *et al.* 2006). The Ag2 atom adopts a close-to-tetrahedral

TABLE 3. ATOMS, WYCKOFF LETTER, SITE OCCUPANCY, FRACTIONAL ATOM COORDINATES (Å), AND ATOMIC DISPLACEMENT PARAMETERS (Å<sup>2</sup>) FOR TE-RICH CANFIELDITE

Atom	Wyckoff	Site Occupancy	x	y	z	$U_{11}$
Sn	4c	$\text{Sn}_{1.00}$	$\frac{1}{4}$	$\frac{1}{4}$	$\frac{1}{4}$	0.0362(4)
Ag1	24f	$\text{Ag}_{0.423}$	0.2217(1)	0	0	0.0460(9)
Ag2	48h	$\text{Ag}_{0.455}$	0.42938(6)	0.42938(6)	0.76192(9)	0.0465(4)
X1	16e	$\text{S}_{0.580(9)}\text{Te}_{0.420}$	0.37500(6)	0.37500(6)	0.37500(6)	0.0502(7)
X2	4a	$\text{S}_{0.782(7)}\text{Te}_{0.218}$	0	0	0	0.049(1)
X3	4d	$\text{S}_{0.795(7)}\text{Te}_{0.205}$	$\frac{3}{4}$	$\frac{3}{4}$	$\frac{3}{4}$	0.049(1)

Atom	$U_{22}$	$U_{33}$	$U_{23}$	$U_{13}$	$U_{12}$	$U_{iso}$
Sn	0.0362(4)	0.0362(4)	0	0	0	0.0362(4)
Ag1	0.0457(6)	0.0457(6)	-0.0001(7)	0	0	0.0458(4)
Ag2	0.0465(4)	0.0465(6)	0.0001(3)	0.0001(3)	0	0.0465(4)
X1	0.0502(7)	0.0502(7)	0.0002(3)	0.0002(3)	0.0002(3)	0.0502(7)
X2	0.049(1)	0.049(1)	0	0	0	0.049(1)
X3	0.049(1)	0.049(1)	0	0	0	0.049(1)

coordination (Fig. 3) with an overall mean Ag-X distance of 2.76 Å, which is slightly larger than those found for the pearceite-polybasite group of minerals (range: 2.68-2.72 Å; Bindi *et al.* 2006, 2007, Evain *et al.* 2006) and that observed for the Ag(3) position in the crystal structure of stephanite, Ag<sub>5</sub>[SbS<sub>3</sub>] (2.68 Å; Ribár & Nowacki 1970). Neither the Ag1 nor the Ag2 polyhedra, however, exhibit the expected marked lengthening of the bond distances (due to the presence of large amounts of Te replacing S) or differences in the Ag-X distances with X having different S/Te ratios. Indeed, the refinement of the site-occupancy factors indicated Te to be disordered among the three anion positions (*i.e.*, X1, X2, and X3), with a preference for the X1 site (Table 3). This preference, however, is not driven by any intrinsic difference in the anion environment. We believe that the discrepancies noted above are unlikely to be related to errors in the occupancy factors. On the contrary, they could be related to the fact that both the silver positions are partially occupied and the amount of vacancy at these sites could play a role in the shortening of the bond distances.

Finally, the Sn position shows a regular tetrahedral coordination (Fig. 2), with a mean bond distance of 2.382 Å. This value is much longer than the “tetrahedral” Ge-S distance observed in putzite (2.192 Å; Paar *et al.* 2004). This is obviously due to the larger ionic radius of Sn with respect to Ge (0.55 Å vs. 0.39 Å; Shannon 1981) and to the Te → S substitution occurring in Te-rich canfieldite.

#### DISCUSSION

We have interpreted the Te-rich canfieldite structure as a disordered structure in which the coordination polyhedra are statistically occupied in order to avoid short metal-metal contacts. Such a feature is strongly related to the difficulty in describing the atom electron density of silver. Indeed, silver easily adopts various complex

TABLE 4. SELECTED BOND DISTANCES (Å)  
FOR Te-RICH CANFIELDITE

Sn	–	X3 (×4)	2.382(1)
Ag1	–	X2	2.438(2)
	–	X1 (×2)	2.574(1)
mean			2.529
Ag2	–	X1 (×2)	2.694(1)
	–	X3	2.794(1)
	–	X2	2.840(1)
mean			2.756

TABLE 5. CALCULATED X-RAY POWDER-DIFFRACTION  
DATA FOR Te-RICH CANFIELDITE

I	$d_{calc}$	h	k	l
4.93	6.3510	1	1	1
14.34	3.3167	3	1	1
100.00	3.1755	2	2	2
9.74	2.7501	4	0	0
12.55	2.5236	3	3	1
2.74	2.4597	4	2	0
12.73	2.2454	4	2	2
23.32	2.1170	5	1	1
20.54	2.1170	3	3	3
29.33	1.9446	4	4	0
25.61	1.8594	5	3	1
7.17	1.8334	6	0	0
2.37	1.6775	5	3	3
5.76	1.6584	6	2	2
3.68	1.5404	7	1	1
2.65	1.4321	5	5	3
2.24	1.3750	8	0	0
7.03	1.2964	6	6	0
3.82	1.2964	8	2	2
3.07	1.2702	5	5	5
4.74	1.2618	6	6	2
2.13	1.2074	9	1	1
4.81	1.2074	7	5	3
3.82	1.2002	8	4	2
2.66	1.1531	9	3	1
9.16	1.1227	8	4	4
2.41	1.0585	10	2	2
2.38	1.0585	6	6	6
3.49	0.9611	11	3	1
3.34	0.9575	8	8	2
3.00	0.9433	10	6	0
2.79	0.9297	10	6	2
2.34	0.8836	9	7	5
5.35	0.8697	12	4	0
2.17	0.8412	13	1	1
2.41	0.8412	11	5	5
2.44	0.8412	9	9	3
2.65	0.8388	10	6	6
4.68	0.8222	11	7	3
2.72	0.8199	12	6	0
4.94	0.8044	9	9	5
2.00	0.8044	13	3	3
6.08	0.7939	8	8	8
2.96	0.7877	13	5	1
2.71	0.7877	11	7	5
2.50	0.7857	12	6	4
3.44	0.7778	10	10	0
14.50	0.7721	11	9	1
11.56	0.7721	13	5	3

Note: The calculated X-ray powder pattern was computed on the basis of a 11.0003(6) Å and with the atomic coordinates and occupancies reported in Table 3.

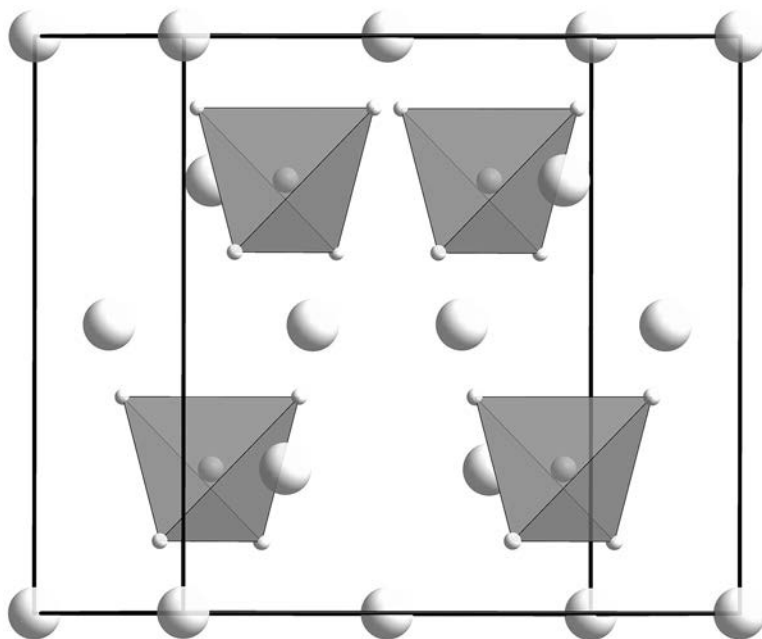


FIG. 2. The crystal structure of Te-rich canfieldite down [001] (perspective view). The  $\text{SnS}_4$  tetrahedra are shown in grey. S atoms are represented as white circles. Ag atoms are not shown for clarity. The unit cell is outlined.

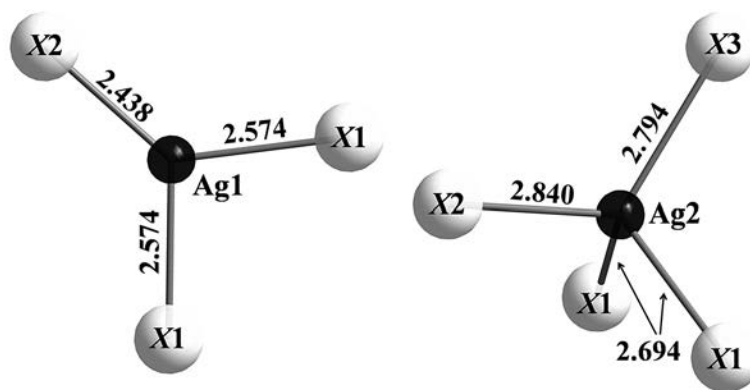


FIG. 3. Crystal-chemical environments of the Ag1 and Ag2 atoms (black circles).

asymmetric coordinations. It has been shown (Gaudin *et al.* 2001 and references therein) that those coordinations are due to an *s-d* orbital mixing or polarization factors. Therefore, it is quite common to observe, in a space and time average, Ag in different, but very close sites. This certainly also favours the presence of strong ionic conductivity observed in argyrodite-type compounds

(Rao & Adams 2011), for which there exists a delocalization of an ionic species over a liquid-like structure.

The Ag disorder in argyrodite-type compounds is usually approached with the use of higher-order tensor elements in the expression of the structure factors (the “non harmonic approach” of Johnson & Levy 1974, Zucker & Schulz 1982) rather than the

classical split-atom model. This alternative approach, in particular the Gram-Charlier formalism (Trueblood *et al.* 1996), provides an easier convergence of the refinement due to much lower correlations between the refined parameters. We tried to apply the Gram-Charlier formalism to Te-rich canfieldite (by means of the program JANA2006; Petříček *et al.* 2006), but we observed large negative regions in the probability-density functions (*pdf*), indicating some inadequacy of the results. Thus, we turned to the use of the split-atom model to mimic the electron density of silver, since the simultaneous refinement of overlapping atoms with partial occupancy (*i.e.*, Ag1 and Ag2) did not give rise to high correlations and unstable refinements. As is well known, in some situations it is better to use only the Gaussian approximation, even though the resulting *R* factors may be higher.

Finally, it is interesting to note that Te-rich canfieldite shows a cubic structure, space group  $F\bar{4}3m$ , as observed for the putzite structure (Paar *et al.* 2004). In general, low-temperature modifications of argyrodite-group compounds are orthorhombic, whereas high-temperature modifications may attain cubic symmetry. Indeed, the mineral argyrodite is reported as orthorhombic, space group  $Pna2_1$  (Eulenberger 1977). On the other hand, no structural studies of natural canfieldite have confirmed it to be isostructural with argyrodite, although it is commonly reported with the space group  $Pna2_1$  in several mineralogical databases (*e.g.*, Strunz & Nickel 2001). Moreover, DTA studies carried out by Gorochov (1968) on synthetic  $Ag_8SnS_6$  and  $Ag_8GeS_6$  have revealed reversible phase-transitions from an orthorhombic low-temperature modification to a cubic one at 172 and 223 °C, respectively. We cannot infer that the crystal structure of pure canfieldite (without tellurium) is cubic as well, but we can state that Te-rich canfieldite shows a fully disordered structure stable at room temperature. It could convert to an ordered form at low temperature, where the order could give rise to an orthorhombic unit-cell as observed for the mineral argyrodite (Eulenberger 1977). However, this mechanism needs to be confirmed through the elucidation of the structure of Te-rich canfieldite at a low temperature, which is currently in progress.

#### ACKNOWLEDGEMENTS

The paper benefited from the official reviews made by Stuart Mills, Allan Pring, and Associate Editor Allen Pratt. Authors are also grateful to the Editor, Robert F. Martin, for his suggestions on improving the manuscript. This work was funded by “Progetto d’Ateneo 2006” to F. Nestola. R. Carampin is thanked for the WDS analyses, whereas L. Tauro and E. Masiero helped with sample preparation.

#### REFERENCES

- BINDI, L., EVAIN, M. & MENCHETTI, S. (2006) Temperature dependence of the silver distribution in the crystal structure of natural pearceite,  $(Ag,Cu)_{16}(As,Sb)_2S_{11}$ . *Acta Crystallographica* **B62**, 212-219.
- BINDI, L., EVAIN, M. & MENCHETTI, S. (2007) Complex twinning, polytypism and disorder phenomena in the crystal structures of antimonpearceite and arsenopolybasite. *Canadian Mineralogist* **45**, 321-333.
- DUDA, R. & KRISTIN, J. (1978) Telluride mineralisation occurrence on the Zlata Bana locality (Slanské vrchy Mountains, eastern Slovakia). *Mineralia Slovaca* **10**, 47-53.
- ENGEL, P. & NOWACKI, W. (1966) Die Verfeinerung der Kristallstruktur von Proustit,  $Ag_3AsS_3$ , und Pyrargyrit,  $Ag_3SbS_3$ . *Neues Jahrbuch für Mineralogie-Monatshefte* **1966**, 181-195.
- EULENBERGER, G. (1977) Die kristallstruktur der tiefemperaturmodifikation von  $Ag_8GeS_6$ . *Monatshefte für Chemie* **108**, 901-913.
- EVAIN, M., BINDI, L. & MENCHETTI, S. (2006) Structural complexity in minerals: twinning, polytypism and disorder in the crystal structure of polybasite,  $(Ag,Cu)_{16}(Sb,As)_2S_{11}$ . *Acta Crystallographica* **B62**, 447-456.
- EVAIN, M., GAUDIN, E., BOUCHER, F., PETRÍČEK, V. & TAULELLE, F. (1998) Structures and phase transitions of the  $A_7PSe_6$  ( $A = Ag,Cu$ ) argyrodite-type ionic conductors. I.  $Ag_7PSe_6$ . *Acta Crystallographica* **B54**, 376-383.
- GAUDIN, E., BOUCHER, F. & EVAIN, M. (2001) Some factors governing  $Ag^+$  and  $Cu^+$  low coordination in chalcogenide environments. *Journal of Solid State Chemistry* **160**, 212-221.
- GOROCHOV, O. (1968) Les composés  $Ag_8MX_6$  ( $M = Si, Ge, Sn$  et  $X = S, Se, Te$ ). *Bulletin de la Societe Chimique de France*, 2263-2275.
- GRAESER, M. (1965) Die Mineralfundstellen im Dolomit des Binnatales. *Schweizer Mineralogische und Petrographische Mitteilungen* **46**, 367-375.
- GRAESER, S., CANNON, R., DRECHSER, E., RABER, T. & ROTH, P. (2008) Faszination Lengenbach abbau - Forschung - Mineralien 1958-2008. Kristallographik Verlag, Achberg, 192 pp.
- HARRIS, D.C. & OWENS, D.R. (1971) A tellurium-bearing canfieldite, from Revelstoke, B.C. *Canadian Mineralogist* **10**, 895-898.
- HOFMANN, B.A. & KNILL, M.D. (1996) Geochemistry and genesis of the Lengenbach Pb-Zn-As-Tl-Ba- mineralization, Binn Valley, Switzerland. *Mineralium Deposita* **31**, 319-339.

- IBERS, J.A. AND HAMILTON, W.C., EDS. (1974) *International Tables for X-ray Crystallography*, vol. IV, 366 pp. Kynock, Dordrecht, The Netherlands.
- ISHII, M., ONODA, M. & SHIBATA, K. (1999) Structure and vibrational spectra of argyrodite family compounds  $\text{Cu}_8\text{SiX}_6$  ( $X = \text{S}, \text{Se}$ ) and  $\text{Cu}_8\text{GeS}_6$ . *Solid State Ionics* **121**, 11-18.
- JOHNSON, C.K. & LEVY, H.A. (1974) *International Tables for X-ray Crystallography*, edited by J. A. Ibers and W. C. Hamilton, Vol. IV, pp. 311-336. Birmingham: Kynoch Press.
- KIKUCHI, Y., MATSUEDA, H. & MATSUKUMA, T. (1980) On the mineral association of ore minerals at the Kuga mine. Japanese Association of Mineralogists, Petrologists and Economic Geologists, Mineralogical Society of Japan, and Society of Mining Geologists of Japan. Sapporo, Japan.
- MARIOKO, T. (1981) Silver distribution and silver-bearing minerals in the Nakayama and Hitokata ore deposits of the Nakatatsu mine, Fukui Prefecture, Japan. *Mining Geology, Special Issue* **10**, 159-179.
- MILÉSI, J.P., MARCOUX, E., NEHLIG, P., SUNARYA, Y., SUKANDAR, A. & FELENC, J. (1994) Cirotan, West Java, Indonesia: a 1.7 Ma hybrid epithermal Au-Ag-Sn-W deposit. *Economic Geology* **89**, 227-245.
- NESTOLA, F., GUASTONI, A., BINDI, L. & SECCO L. (2010) Dalnegroite,  $\text{Tl}_{5-x}\text{Pb}_{2x}(\text{As,Sb})_{21-x}\text{S}_{34}$ , a new thallium sulphosalt from Lengenbach quarry, Binntal, Canton Valais, Switzerland. *Mineralogical Magazine* **73**, 1027-1032.
- ONTOYEV, D.A., TRONEVA, N.V., TSEPIN, A.I. & VYAL'SOV, L.N. (1971) First find of tellurium canfieldite. *Doklady Akademii Nauk, SSSR* **203**, 169-171 (in Russian).
- PAAR, W.H., ROBERTS, A.C., BERLEPSCH, P., ARMBRUSTER, T., TOPA, D. & ZAGLER, G. (2004) Putzite,  $(\text{Cu}_{4.7}\text{Ag}_{3.3})_8\text{GeS}_6$ , a new mineral species, from Capillitas, Catamarca, Argentina: Description and crystal structure. *Canadian Mineralogist* **42**, 1757-1769.
- PETŘÍČEK, V., DUSEK, M. & PALATINUS, L. (2006) JANA2006, Structure Determination Software Programs. Institute of Physics, Academy of Sciences of the Czech Republic, Prague, Czech Republic.
- POUCHOU, J.L. & PICOIR, F. (1985) PAP ( $\phi$ - $\rho$ -Z) procedure for improved quantitative microanalysis. In *Microbeam Analysis* (J.T. Armstrong, ed.). San Francisco Press, San Francisco, pp. 104-106.
- RAO, R.P. & ADAMS, S. (2011) Studies of lithium argyrodite solid electrolytes for all-solid-state batteries. *Physica Status Solidi A* **208**, 1804-1807.
- RIBÁR, B. & NOWACKI, W. (1970) Die Kristallstruktur von Stephanit,  $[\text{SbS}_3]_2[\text{SI}Ag_5^{III}]$ . *Acta Crystallographica B* **26**, 201-207.
- SHANNON, R.D. (1981) *Structure and Bonding in Crystals*, edited by M. O'Keeffe and A. Navrotsky, Vol. II, pp. 53-70. New York: Academic Press.
- SHELDRIK, G.M. (2008) A short history of SHELX. *Acta Crystallographica A* **64**, 112-122.
- SOEDA, A., WATANABE, M., HOSHINO, K. & NAKASHIMA, K. (1984) Mineralogy of tellurium-bearing canfieldite from the Tsumo mine, SW Japan and its implications for ore genesis. *Neues Jahrbuch für Mineralogie- Abhandlungen* **150**, 11-23.
- STRUNZ, H. & NICKEL, E.H. (2001) *Strunz Mineralogical Tables. Chemical-Structural Mineral Classification System*. 9th Ed. Schweizerbart, Stuttgart, Germany.
- TAMAŞ, C.G., BAILLY, L., GHERGARI, L., O'CONNOR, G. & MINUŢ, A. (2006) New occurrences of tellurides and argyrodite in Roşia Montană, Apuseni Mountains, Romania, and their metallogenetic significance. *Canadian Mineralogist* **44**, 367-383.
- TRUEBLOOD, K.N., BÜRGI, H.-B., BURZLAFF, H., DUNITZ, J.D., GRAMACCIOLI, C.M., SCHULZ, H., SHMUELI, U. & ABRAHAMS, S.C. (1996) Atomic Displacement Parameter Nomenclature. Report of a Subcommittee on Atomic Displacement Parameter Nomenclature. *Acta Crystallographica A* **52**, 770-781.
- WANG, N. (1978) New data for  $\text{Ag}_8\text{SnS}_6$  (canfieldite) and  $\text{Ag}_8\text{GeS}_6$  (argyrodite). *Neues Jahrbuch für Mineralogie-Monatshefte* **1978**, 269-272.
- ZUCKER, U.H. & SCHULZ, H.H. (1982) Statistical approaches for the treatment of anharmonic motion in crystals. II. Anharmonic thermal vibrations and effective atomic potentials in the fast ionic conductor lithium nitride ( $\text{Li}_3\text{N}$ ). *Acta Crystallographica A* **38**, 568-576.

Received September 27, 2011, revised manuscript accepted November 18, 2011.